EXECUTIVE SUMMARY

MATHEMATICAL MODELING OF PHOTOCHEMICAL AIR POLLUTION

Gregory J. McRae
William R. Goodin
John H. Seinfeld

Environmental Quality Laboratory
California Institute of Technology
Pasadena, California 91125

Final Report to the

STATE OF CALIFORNIA AIR RESOURCES BOARD

in

Completion of Research Under
ARB Contract Nos. A5-046-87 and A7-187-30

18 June 1982

DISCLAIMER

The statements and conclusions in this report are those of the Contractor and not necessarily those of the State Air Resources Board. The mention of commercial products, their source, or their use in connection with material reported herein is not to be construed as either an actual or implied endorsement of such products.

TABLE OF CONTENTS

LIST OF FIGURES

LIST OF TABLES

1. Introduction

Air pollution is an environmental problem that is both pervasive and difficult to control. An important element of any rational control approach is a reliable means for evaluating the air quality impact of alternative abatement measures. A major focus of the research described in this report has been to develop a capability to describe the production and transport of photochemical oxidants within an urban airshed. This work has been successfully completed and is reported in more detail in McRae (1981), McRae et al. (1982abc), and McRae and Seinfeld (1982).

2. Model Formulation

The combined influences of advection, turbulent diffusion, chemical reaction, emissions and surface removal processes have been incorporated into a series of mathematical models based on the species continuity equation. A schematic representation of the interaction of these elements is shown in Figure 1. Since each model employs common components the simpler forms can be used for rapid screening calculations and the more complex ones for detailed evaluations. This feature is particularly useful to regulatory agencies that must evaluate many different control strategies. Because of the importance of understanding the practical limitations of these models a delineation of the essential assumptions underlying their formulations has been

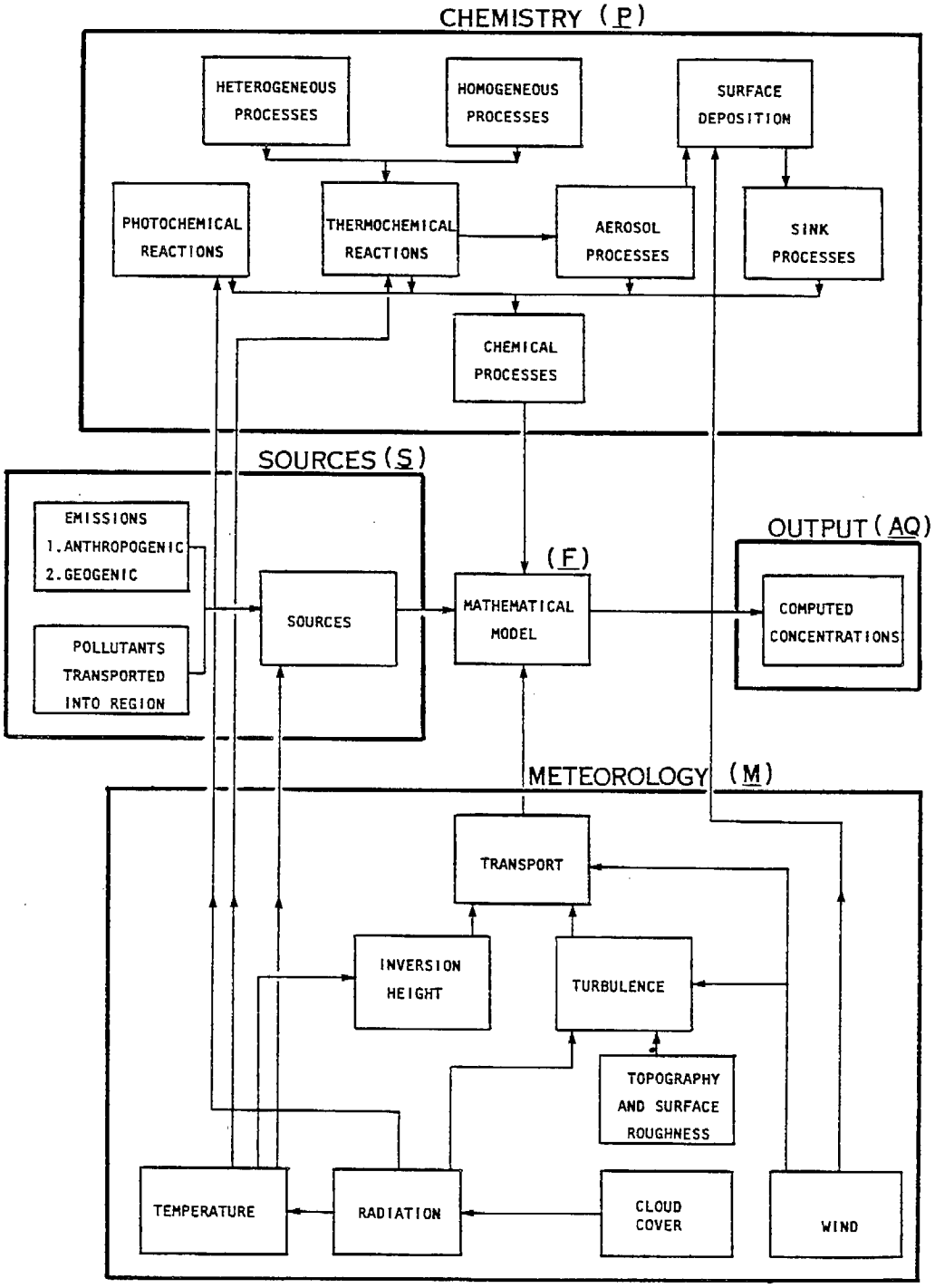

FIGURE 1

Elements of a Mathematical Model for Relating Pollutant Emissions to Ambient Air Quality

carried out. The results of this investigation are reported in Goodin et al. (1979a) and McRae et al. (1982a).

The flow fields, needed for species transport, are constructed using inverse distance weighted polynomial interpolation techniques that map routine monitoring data onto a regular computational mesh (Goodin et al., 1979b; 1981). Variational analysis procedures are then employed to adjust the field so that mass is conserved. These techniques are described in Goodin et al. (1979c) and Goodin and McRae (1980). Initial concentration and mixing height distributions can be established with the same interpolation algorithms.

Subgrid scale turbulent transport is characterized by a gradient diffusion hypothesis. Similarity solutions are used to model the surface layer fluxes. Above this layer different treatments of turbulent diffusivity are required to account for variations in atmospheric stability. Convective velocity scaling is utilized to develop eddy diffusivities for unstable conditions (McRae et al., 1982a). The predicted mixing times are in accord with results obtained during sulfur hexafluoride (SF_6) tracer experiments (McRae et al., 1981). Conventional models are employed for neutral and stable conditions.

A new formulation for gaseous deposition fluxes is presented that provides a means for estimating removal rates as a function of atmospheric stability. The model, described by McRae et al. (1982a), satisfactorily reproduces measured deposition velocities for reactive

materials. In addition it is shown how computational cell size influences the representation of surface removal.

Chemical interactions between twenty nine chemical species are described by a 52 step kinetic mechanism (Falls and Seinfeld, 1978; McRae et al., 1982a). The atmospheric hydrocarbon chemistry is modeled by the reactions of six lumped classes: alkanes, ethylene, other olefins, aromatics, formaldehyde and other aldehydes; a grouping that enables representation of a wide range of smog chamber experiments and atmospheric conditions. Chemical lumping minimizes the number of species while maintaining a high degree of detail for the inorganic reactions. The influence of variations in rate data, stoichiometric coefficients and initial conditions on oxidant production have been studied using the Fourier Amplitude Sensitivity Test (Koda et al., 1979; Falls et al., 1979; McRae et al., 1982d; Tilden et al., 1980 and McRae and Tilden, 1980).

The wide variation in time scales, non-linearity of the chemistry and differences in transport processes complicates selection of numerical algorithms. Operator splitting techniques are used to decompose the governing equation into elemental steps of transport and chemistry. Each transport operator is further split into advective and diffusive components so that linear finite element and compact finite difference schemes can be applied to their best advantage. Because most of the computer time is consumed by the chemical kinetics those species that could be accurately described by pseudo-steady state approximations were identified reducing the number of species,

described by differential equations, to 15. A complete discussion of the numerical techniques can be found in McRae et al. (1982b).

3. Data Base for Model Performance Evaluation

During the week of 23-28 June 1974, a severe air pollution episode was experienced in the South Coast Air Basin of California (Figure 2). Hourly averaged ozone (O_3) concentrations reached 0.50 ppm in the Upland-Fontana area, and values above 0.35 ppm were reported at 10 other stations. These high ozone levels provide a stringent test of the ability of the model to simulate episodes. Another important reason for choosing the 1974 period was that detailed emissions inventories, commissioned by the State of California Air Resources Board, were available for that year.

The basic meteorological input data needed for the model were primarily derived from the South Coast Air Quality Management District (SCAQMD) monitoring stations. During the period 23-28 June, 1974 wind speeds were considerably lower than normal. (Radiosonde data from Pt. Mugu indicated that the wind speeds averaged about 1.6 m s^{-1} between the surface and the 750 mb height; the normal June average is about 4.2 m s^{-1}.)

The mixing height distributions were developed by interpolating acoustic sounder and radiosonde measurements. At El Monte, the maximum depth of the mixed layer was approximately 750 m on each of the days 26-27 June. This value is unseasonably low. Temperatures between the 300 and 900 m levels reached 30°C during 27 and 18 June, while the

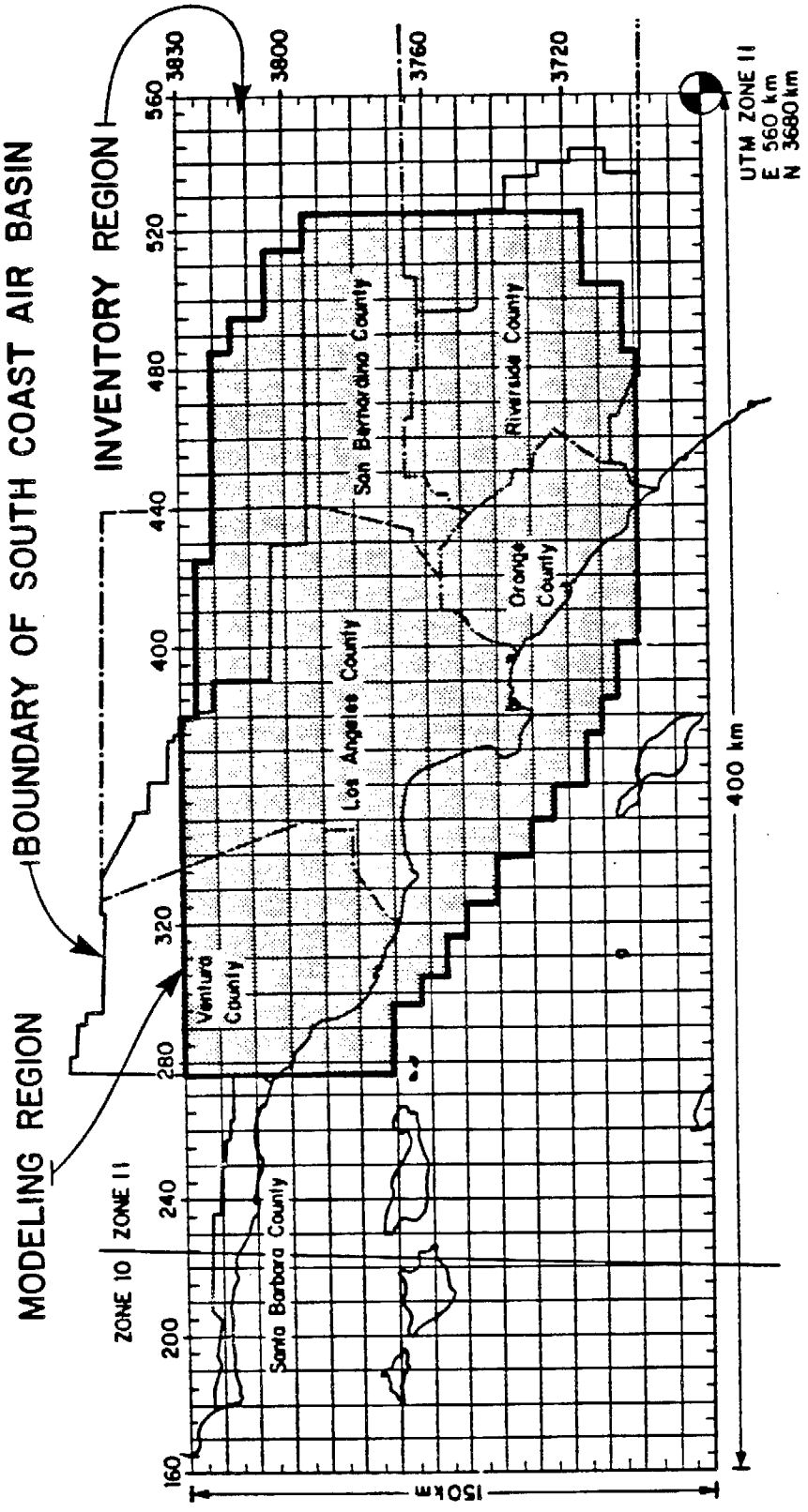

FIGURE 2

Definition of Computational Grid System Over the South Coast Air Basin
The shaded portion corresponds to the area used
in the model performance evaluation.

surface temperatures dropped as low as 15°C during the night. The intense nocturnal inversion was caused partly by subsidence and partly by radiation from the surface since the dry air aloft kept the sky cloudless.

In summary, the low wind speeds, high temperatures and low inversion base produced conditions conducive to the accumulation of precursor emissions and, in turn, to the production of high ozone levels.

One of the most important inputs to any airshed model is a comprehensive detailed and accurate emission inventory, that has been constructed at a level of detail consistent with the required spatial, temporal and chemical resolution of the model. In this study emissions from 130 different source categories were spatially distributed over the region shown in Figure 2. A summary of the daily totals and the distribution between different source classes is shown in Table 1 and Figure 3. Diurnal variations in emission rates were resolved to within one hour in order that the model predictions would be compatible with the averaging time used in making ambient air quality measurements. Table 2 gives the estimated 1974 composition of reactive hydrocarbon emissions in the SCAB grouped according to the six-class chemical lumping scheme. These results were derived from detailed composition profiles developed for each source category. For further details of the emission inventory the reader is referred to McRae et al. (1982c).

TABLE 1

Summary of Estimated 1974 Daily South Coast Air Basin Emissions

SPECIES	TOTAL EMISSIONS (kg/day)	SOURCE CLASS CONTRIBUTION (%) MOBILE	STATIONARY
Carbon monoxide (CO)	8,610,000	98.8	1.2
Nitrogen oxides (NO_x)	1,320,000	62.3	37.7
Sulfur oxides (SO_x)	427,000	13.7	86.3
Total Hydrocarbons (THC)	3,379,000	30.0	70.0
Reactive Hydrocarbons (RHC)	1,290,000	71.0	29.0

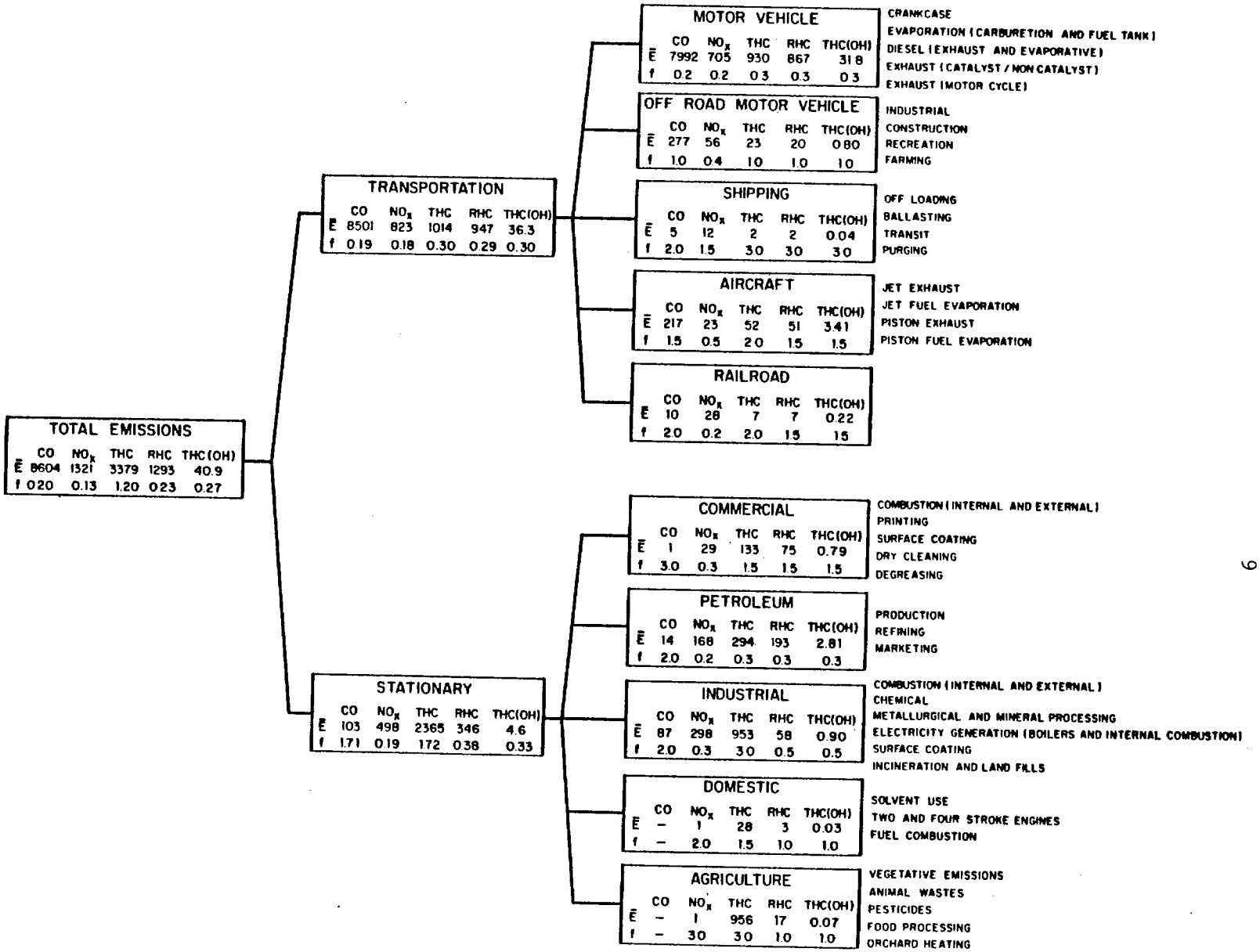

FIGURE 3

Simplified Structure of the Inventory Used in this Study Together with an Assessment of the Uncertainty of Pollutant Emissions from Different Source Categories ($\bar{E}$ is the pollutant emission rate in kg day^{-1}x10^{-3} and f is the fractional uncertainty in the inventory category).

TABLE 2

Composition of Reactive Hydrocarbons in Inventory Region

SPECIES	EMISSIONS $kg\ s^{-1}$	COMPOSITION(%) WEIGHT	MOLE	MOLE WEIGHTED MOLECULAR WEIGHT	AVERAGE CARBON NUMBER
Formaldehyde (HCHO)	0.18	1.25	2.88	30.0	1.00
Other Aldehydes (RCHO)	0.25	1.74	2.22	63.1	3.36
Ethylene (C_2H_4)	0.82	5.73	13.4	28.0	2.00
Other Olefins (OLE)	1.98	13.8	14.2	67.4	4.83
Aromatics (ARO)	2.03	14.2	9.4	100.2	7.56
Alkanes (ALK)	9.04	63.3	57.9	83.5	5.82
TOTALS	14.30	100.0	100.0		

The initial concentration field was established using the procedures described in Goodin et al. (1980). Hourly averaged data from the monitoring sites, shown in Figure 4, were interpolated to the computational grid. Because of the poor quality of most reactive hydrocarbon measurements, a set of splitting factors was developed for converting total hydrocarbon readings into the components needed for the chemical mechanism. These factors were derived from emissions data and from the results of detailed field measurements.

A summary of the aerometric and emissions data compiled for use in this study is presented in Table 3.

4. Model Performance Evaluation

While the mathematical formulation of the complete system contains no regional or area specific information, performance evaluation studies were carried out using data measured in the South Coast Air Basin of Southern California (McRae, 1981; McRae et al., 1982c and McRae and Seinfeld, 1982).

The model was applied to simulate the two-day period 26-27 June 1974 in the SCAB. The concentrations of 15 species were predicted in each computational grid cell as a function of time commencing at 0:00 hours 26 June. Of the 15 species calculated, the two that provide the most stringent test of a model are NO_2 and O_3. Figures 5-9 show predicted and observed concentrations of NO_2 and O_3 during 26-27 June 1974 at several monitoring stations in the SCAB.

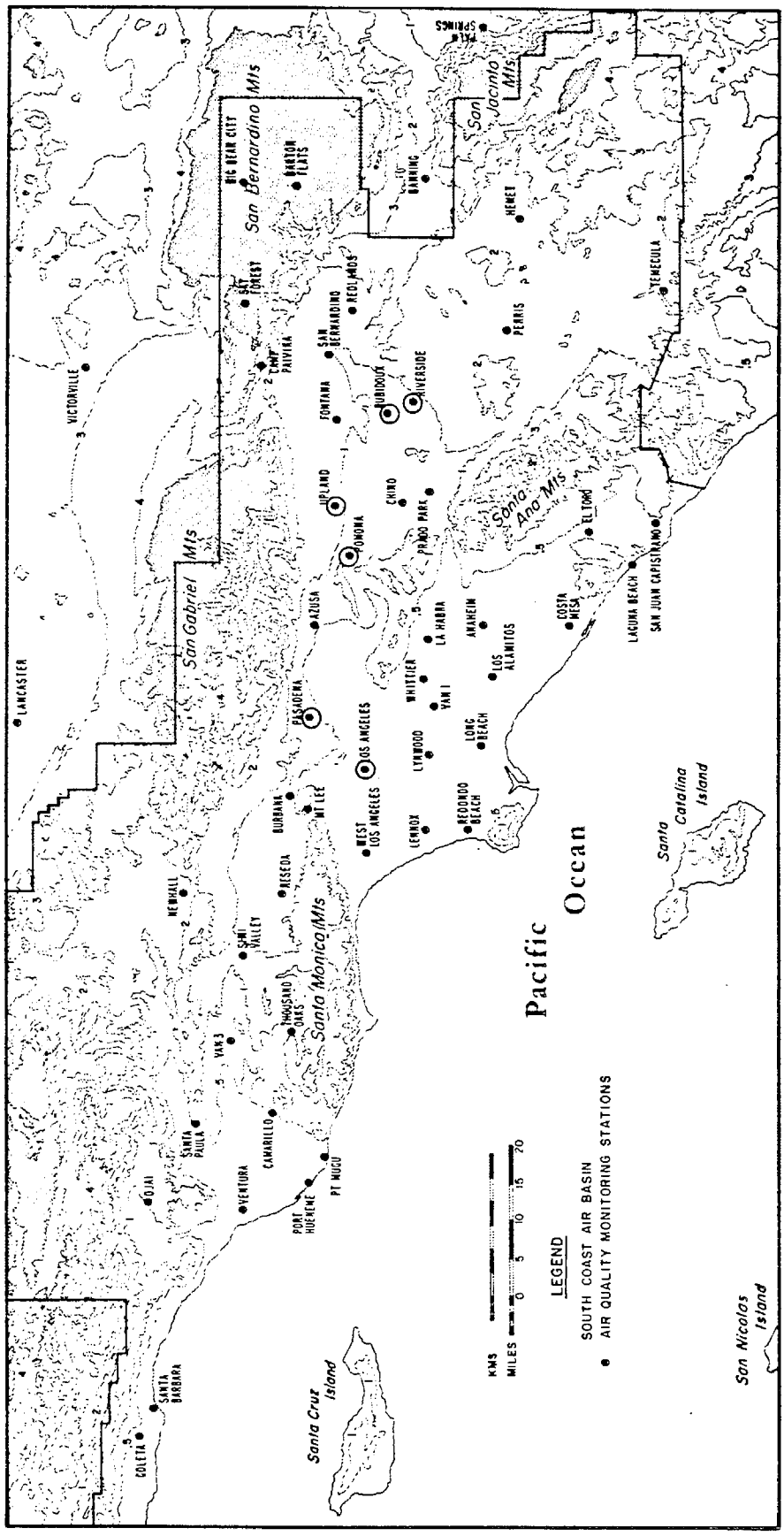

FIGURE 4

Location of Air Quality Monitoring Stations in the South Coast Air Basin
(Air quality predictions and observations at the circled locations are shown in Figures 5-9)

Table 3. Summary of Aerometric and Emissions Information Available for 26-28 June 1974 for the South Coast Air Basin

TYPE OF DATA	NATURE OF DATA COLLECTED	REMARKS	SOURCE OR ORGANIZATION(S) COLLECTING DATA
AIR QUALITY DATA			
Surface pollution concentration	55 air quality monitoring stations	Data are hourly averaged and include measurements of CO, NO, NO_2, O_3, THC, RHC and SO_2.	SCAQMD, ARB, CALTRANS, USFS
Pollution concentrations aloft	None	Estimates of vertical concentration profiles were derived from detailed field measurements collected from different periods.	
METEOROLOGICAL DATA			
Surface Winds	63 surface wind monitoring stations	Data include hourly averaged and instantaneous values.	SCAQMD, ARB, NWS, USN, USAF
Upper level winds	Radiosondes at Edwards AFB (0400 PST), Pt. Mugu (0400, 1000, and 1500 PST), and San Nicholas Island (0930 and 1500 PST). Pibals at LAX (0530 and 1130 PST) and El Monte (0600 and 1230 PST). Aircraft spiral at Riverside (0600 PST).		SCAQMD, USN, USAF, NWS
Mixing depths	Aircraft spiral at Riverside (0600 PST). Radiosondes at LAX (0530, 1030 PST), El Monte (0600, 1230 PST), Pt. Mugu (0400, 1000, 1500 PST), and San Nicholas Island (0930, 1500 PST), and Edwards AFB (0400 PST). Continuous acoustic sounder at El Monte.	Data are instantaneous except for continuous acoustic sounder at El Monte.	ARB, NWS, USN, USAF
Surface temperatures	Temperatures at 14 stations.	Data are hourly averaged values.	NWS, SCAQMD
Solar radiation	Radiation measurements at UCLA and LAX.	Data are hourly averaged and daily averaged values.	NWS, SCAQMD
Humidity	Humidity at 14 stations	Data are hourly averaged values	NWS, SCAQMD
Cloud cover	Cloud cover at 7 airports and 2 other locations.	Data are instantaneous values recorded every hour.	NWS, SCAQMD
EMISSIONS DATA			
Traffic	Emissions estimates derived from the LARTS transportation model and the ARB FWY011 emissions model.	Peak, off-peak and total emissions rates for THC SO_2, NO_x and CO are available. Percentage of hot and cold starts are included in the inventory, but they are not spatially or temporally distributed; vehicle speed distributions and types (four classes) are included.	ARB, CALTRANS
Refinery	Emissions for organic gases, NO_x, CO and particulates estimated for 28 facilities		SCAQMD

Table 3. Summary of Aerometric and Emissions Information Available for 26-28 June 1974 for the South Coast Air Basin (Continued)

TYPE OF DATA	NATURE OF DATA COLLECTED	REMARKS	SOURCE OR ORGANIZATION(S) COLLECTING DATA
EMISSIONS DATA (Cont)			
Aircraft	Gridded emissions estimates for all major airports in inventory region.		CALTRANS, SCAQMD
Power plants	Emissions estimates of NO, NO_2 and CO for each plant in inventory region.	Diurnal distribution of emissions based on inspection of daily operating logs.	SCE, LADWP
Distributed area sources	Emissions estimates for organic gases, NO_x and CO.		SCAQMD
Other stationary sources	Emissions estimates for organic gases, NO_x and CO.		SCAQMD

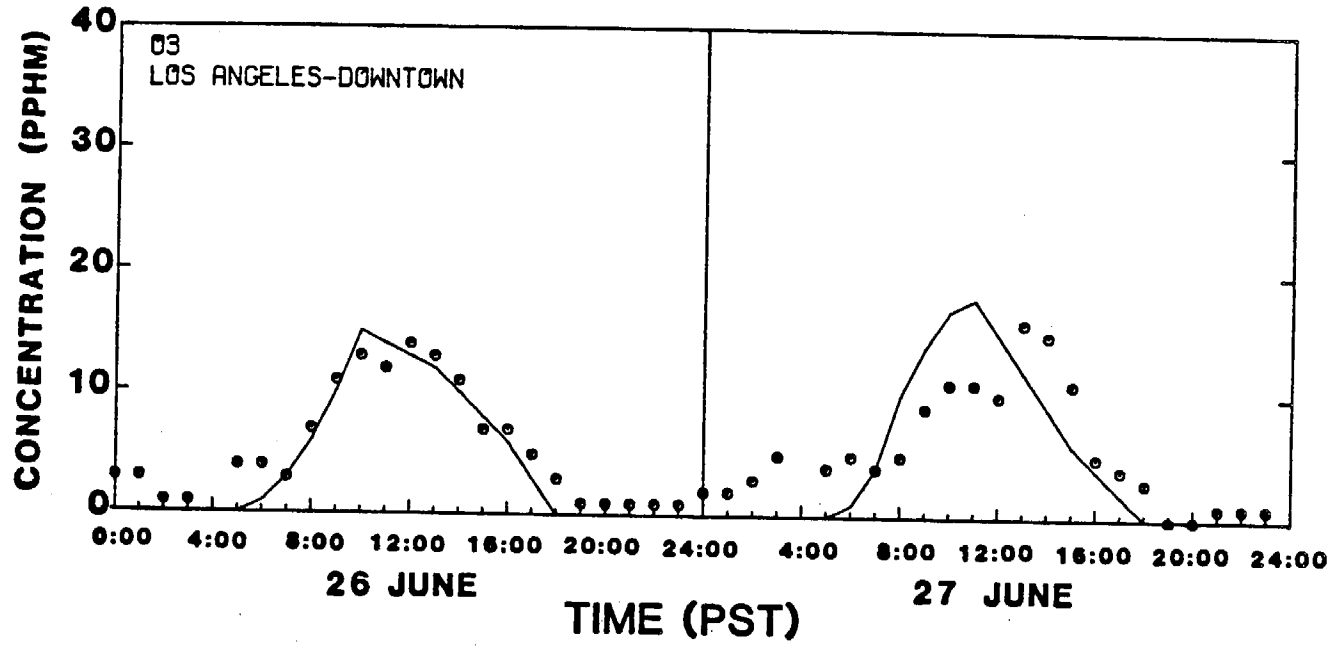

(a)

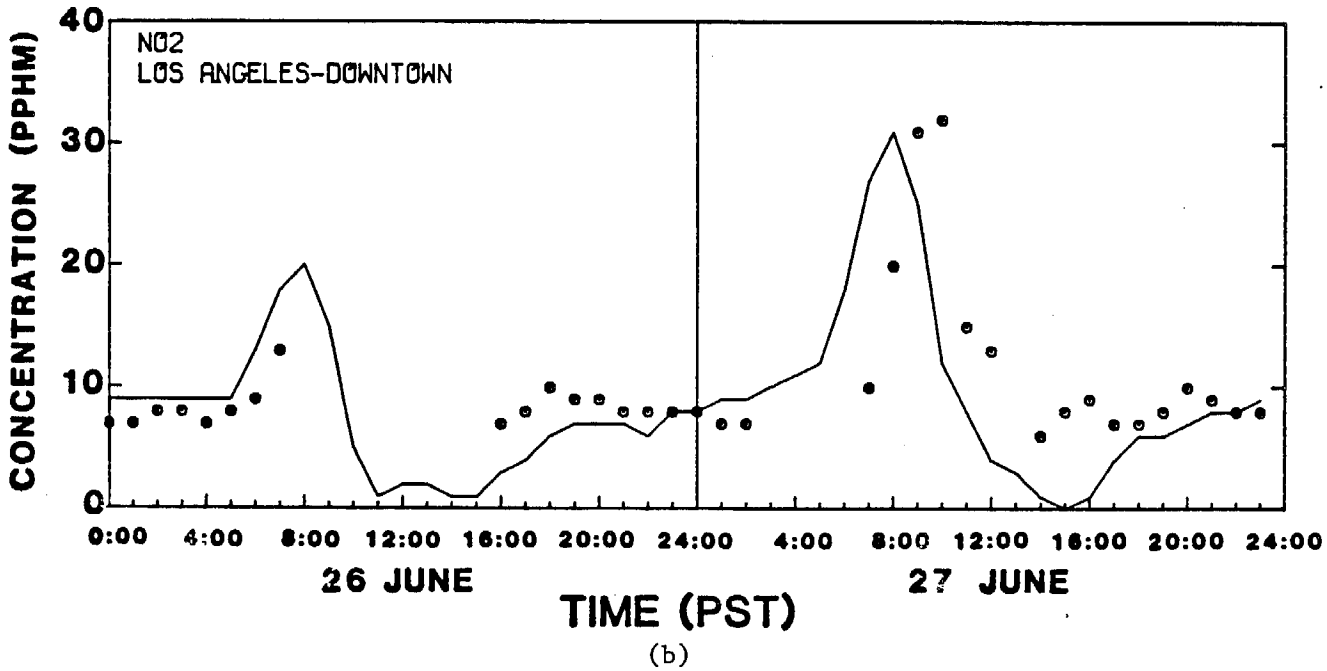

(b)

FIGURE 5

Predicted and Observed Concentrations of:
(a) Ozone and (b) Nitrogen Dioxide at Downtown Los Angeles
(- predicted, o observed)

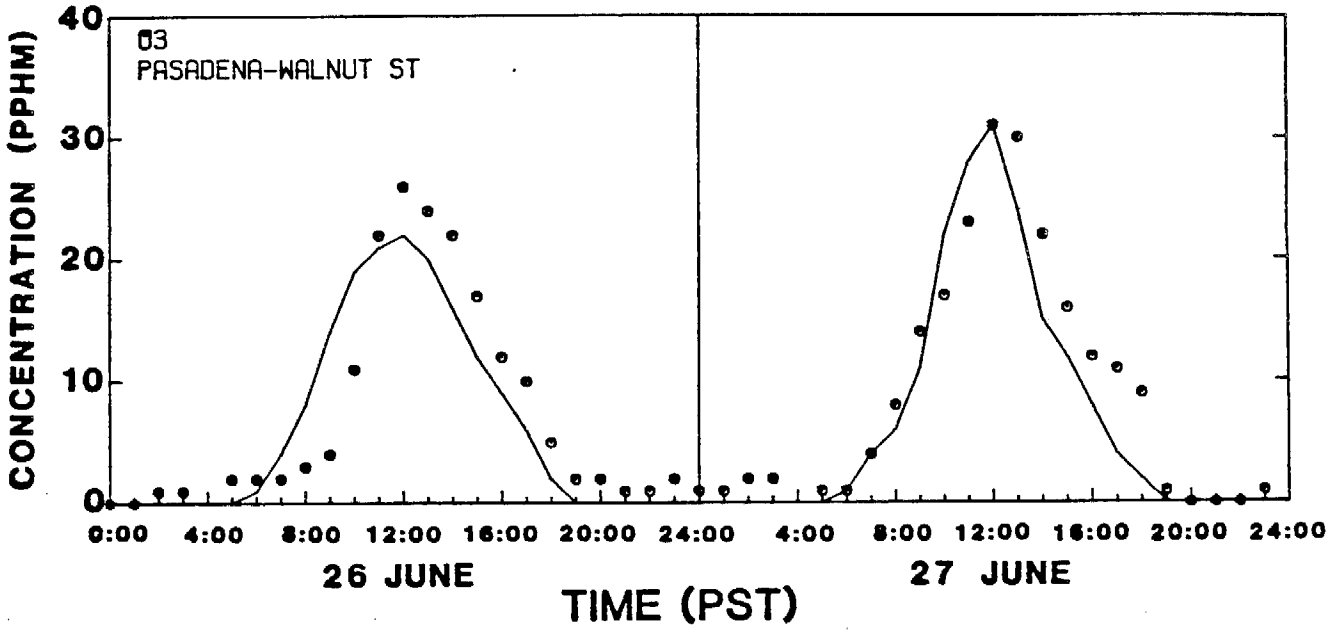

(a)

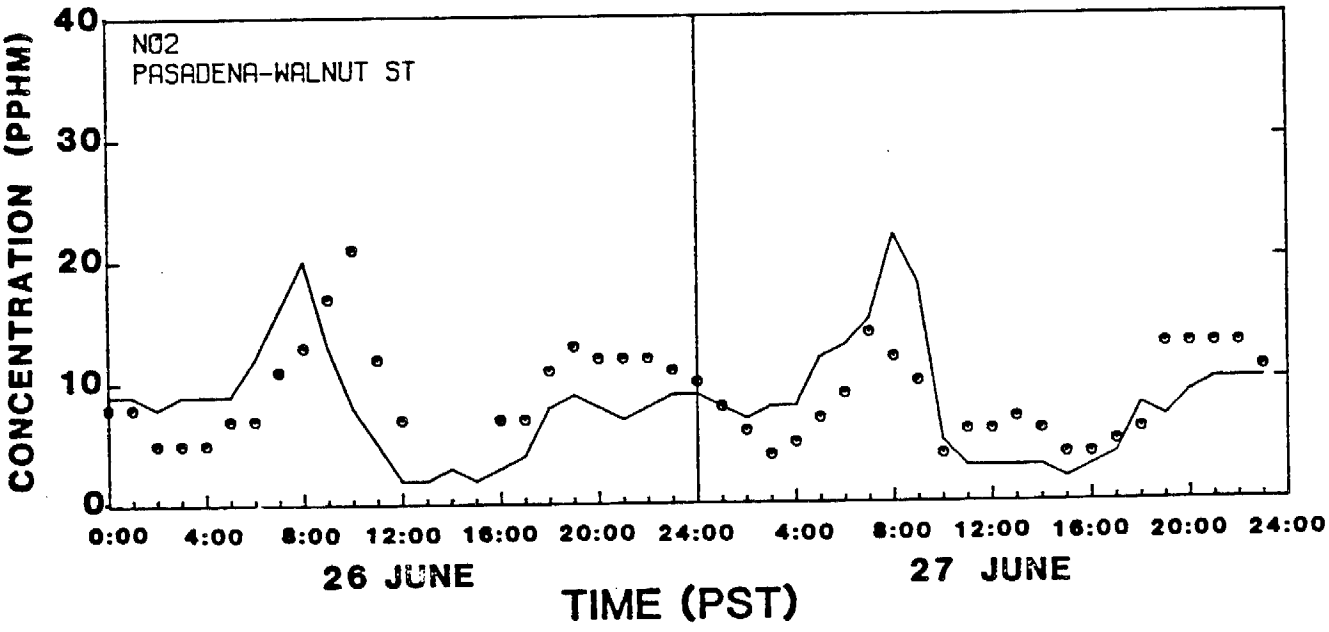

(b)

FIGURE 6

Predicted and Observed Concentrations of:
(a) Ozone and (b) Nitrogen Dioxide at Pasadena
(- predicted, o observed)

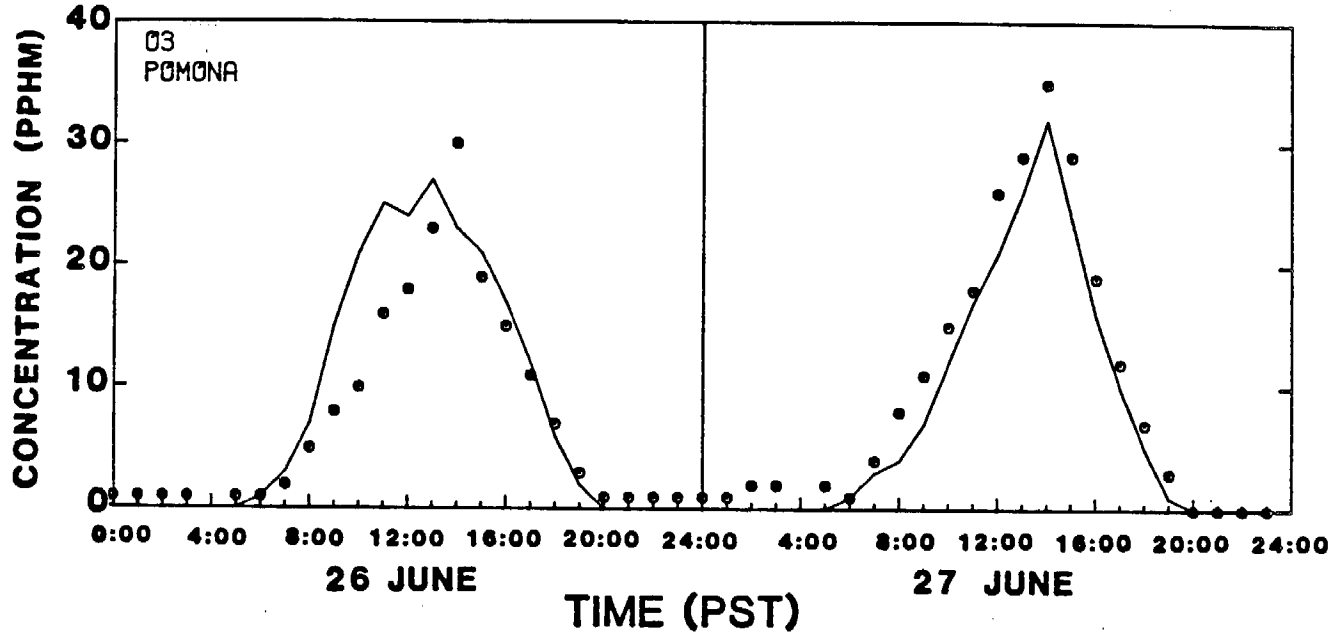

(a)

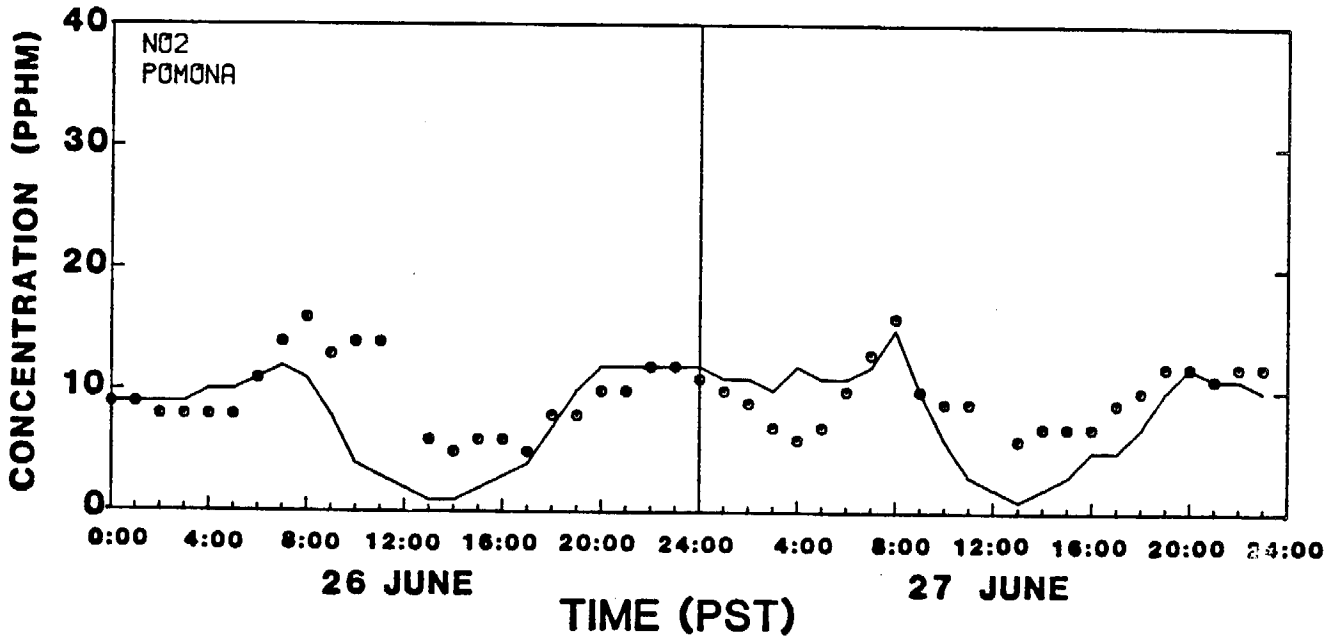

(b)

FIGURE 7

Predicted and Observed Concentrations of:
(a) Ozone and (b) Nitrogen Dioxide at Pomona
(- predicted, o observed)

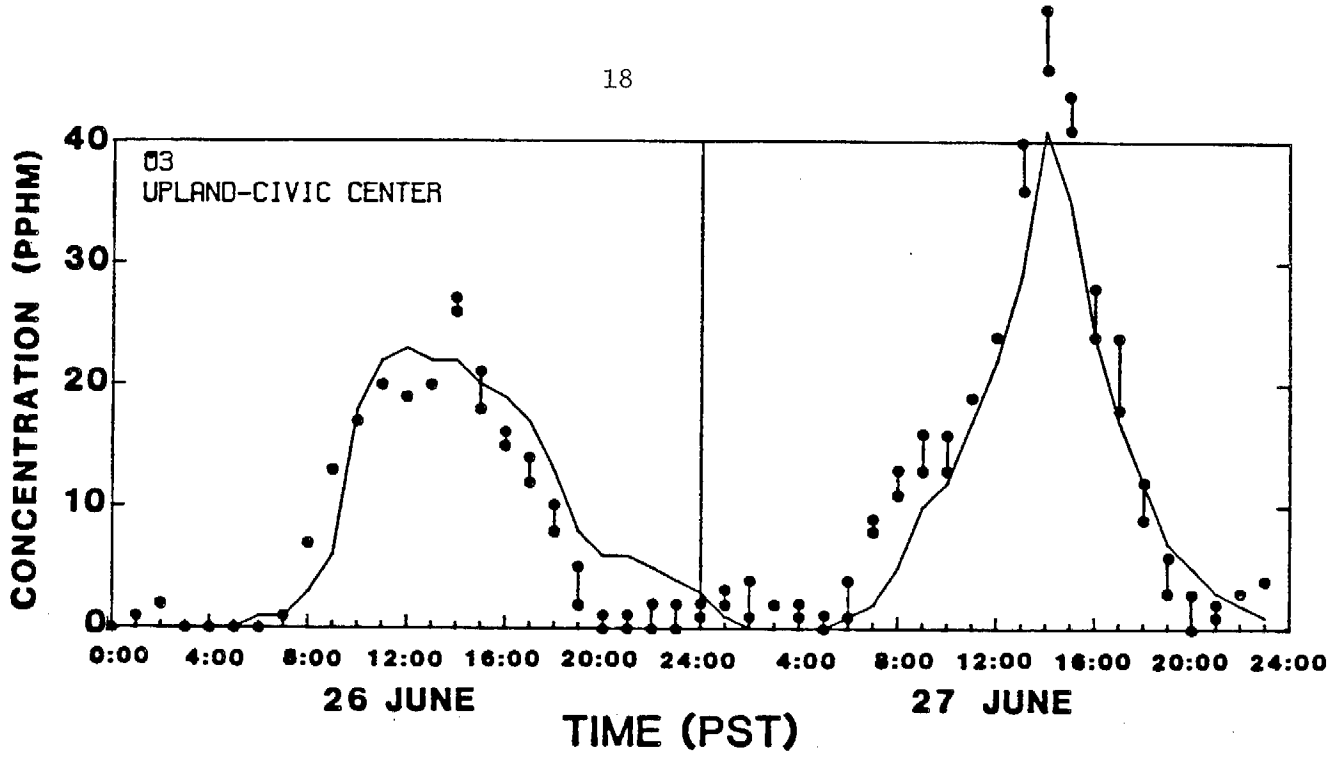

(a)

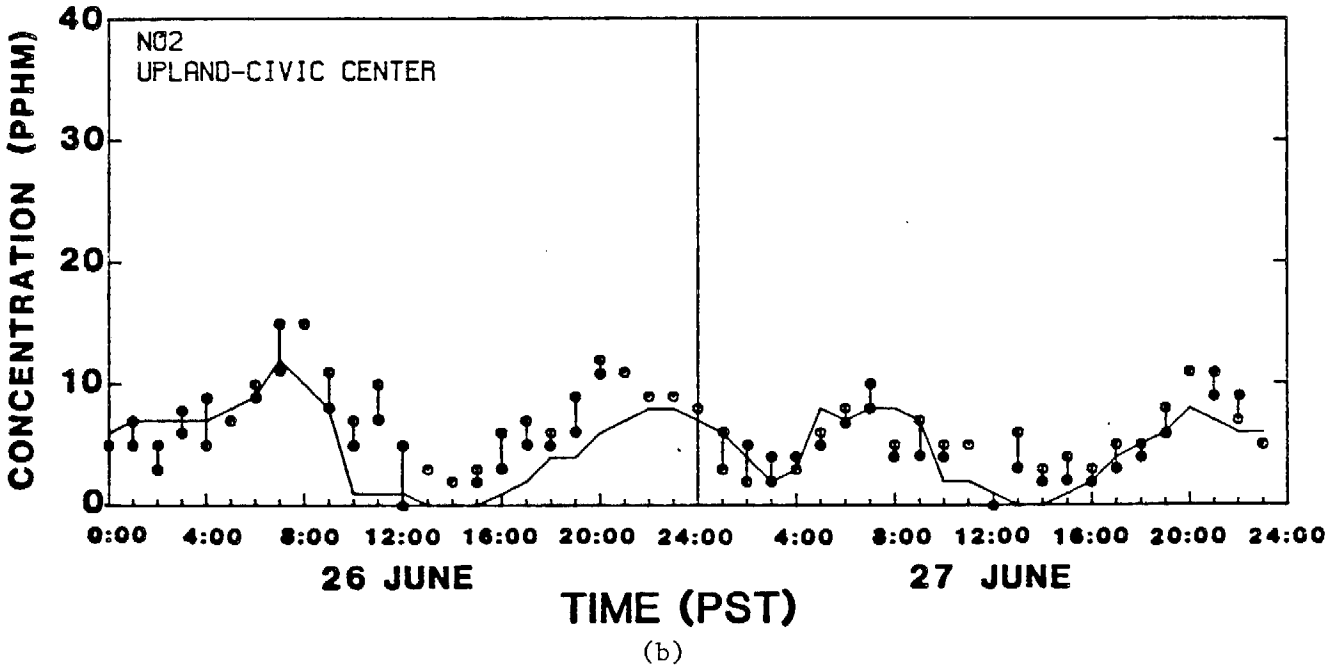

(b)

FIGURE 8

Predicted and Observed Concentrations of:
(a) Ozone and (b) Nitrogen Dioxide at Upland
(- predicted, o observed at CARB station,
• observed at APCD monitoring site located 400 meters away).

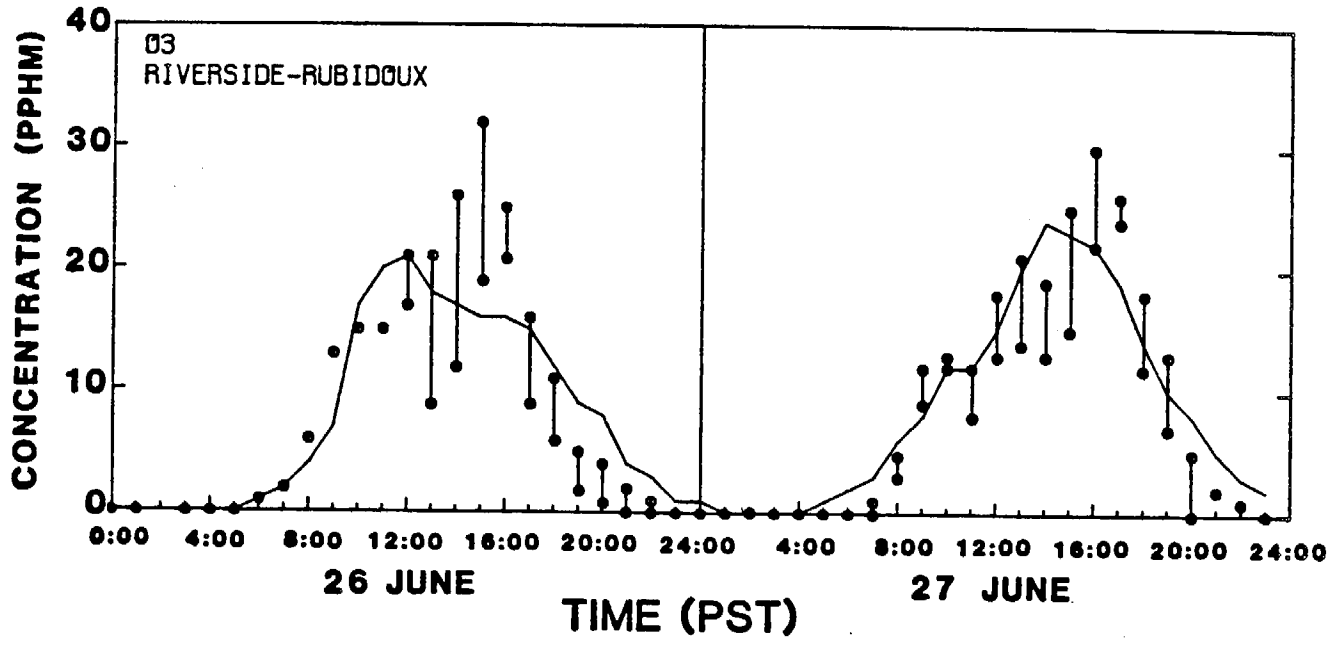

(a)

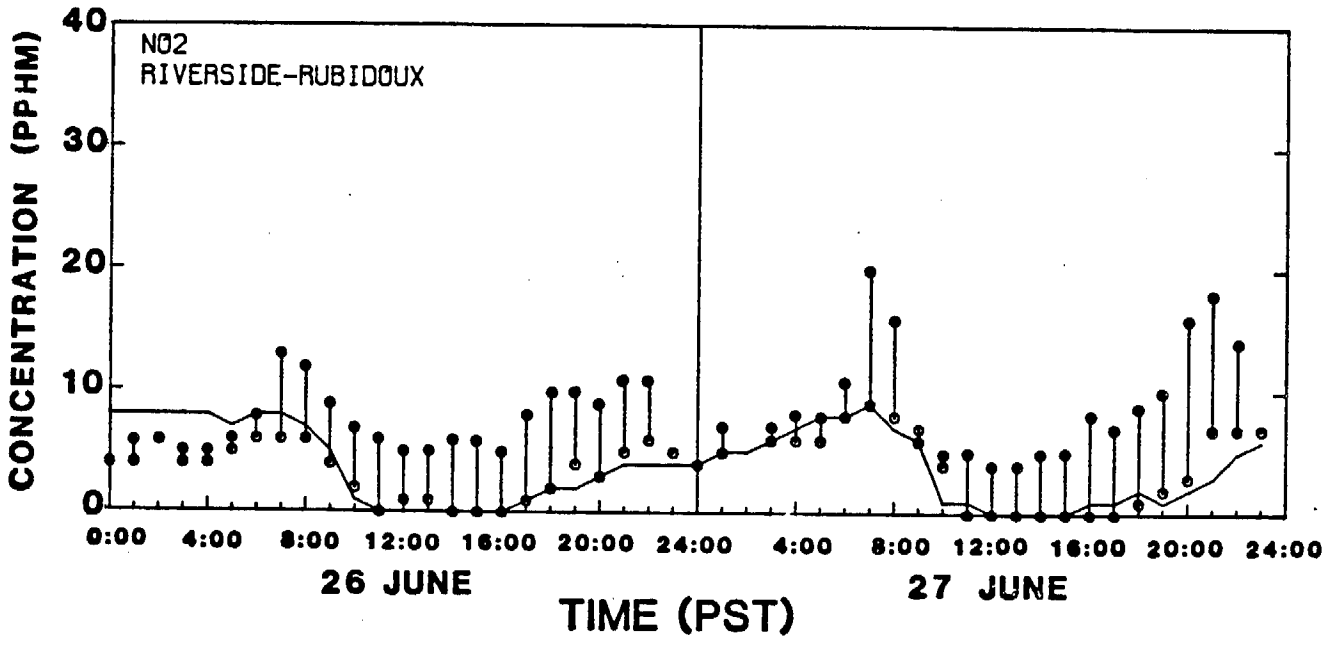

(b)

FIGURE 9

Predicted and Observed Concentrations of:
(a) Ozone and Nitrogen Dioxide at Riverside
(- predicted, o observed at APCD station,
• observed at ARB monitoring site located 1200 meters away).

In the early morning both NO and reactive hydrocarbons peak due to traffic emissions. The NO_2 peak concentrations are delayed a few hours, consistent with the time required to oxidize NO. Observed and predicted ozone concentrations increase with distance toward the east. Ozone concentrations gradually increase until the time of the peak predicted concentration, which usually occurs between 1300 and 1400 PST.

In most cases the model accurately reproduced both the magnitude and timing of the peak ozone concentration. Similar behavior was also noted for nitrogen dioxide except that the model tended to predict the peak values one to two hours earlier. The fact that the model satisfactorily described the observed concentration trends on the second day is particularly encouraging for control strategy calculations. The reason for this is that by running the model for a period longer than the characteristic ventilation time of the airshed it is possible to minimize the influence of uncertainties in specifying the initial conditions. This capability is important for those situations where it is not possible to derive starting conditions from ambient monitoring data.

In many respects a statistical analysis of the deviations between predictions and observations is the heart of model performance evaluation. Although raw statistical comparison of observed and predicted values may not reveal the cause of discrepancies, it can tell much about the nature of the mismatch. Figure 10 shows the frequency distribution of the residuals, i.e. predicted concentrations minus

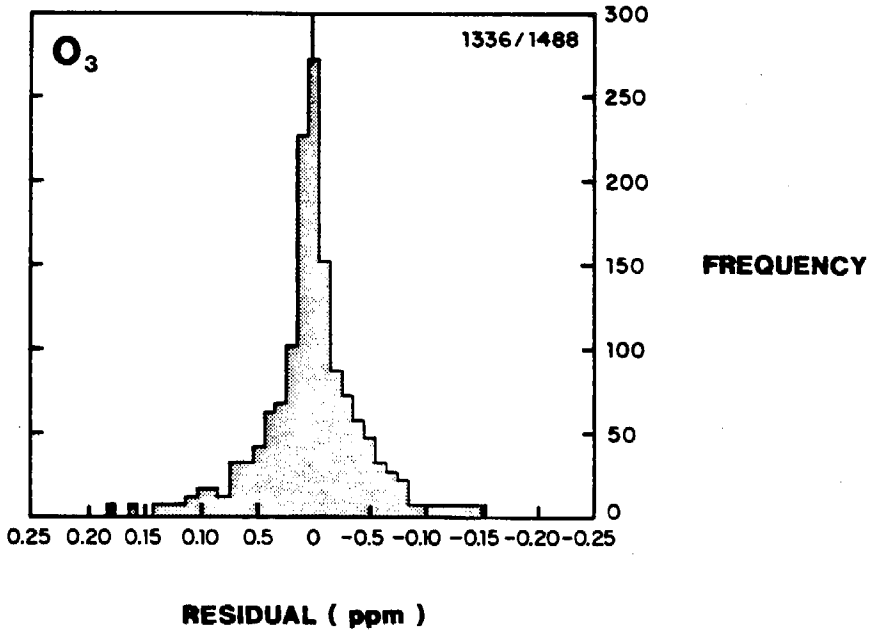

(a)

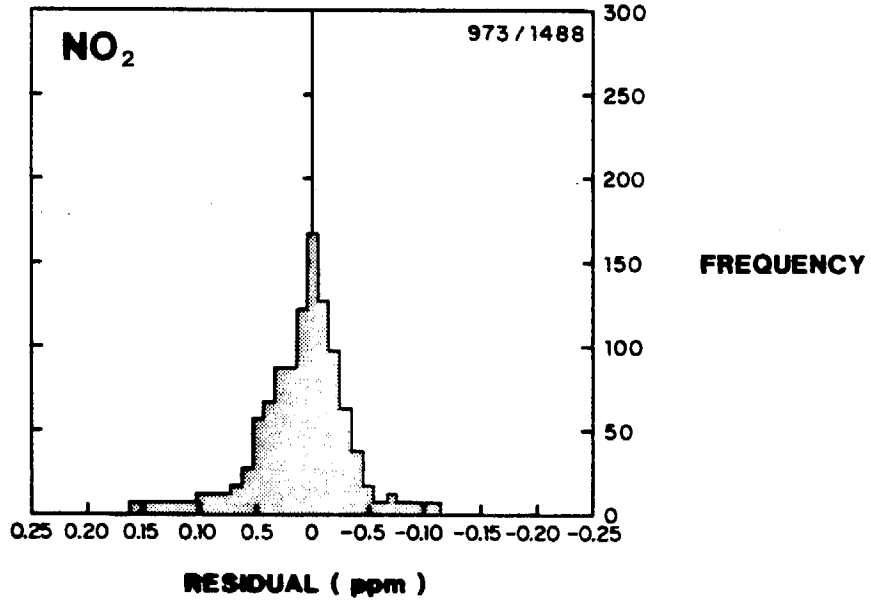

(b)

FIGURE 10

Histograms of Concentrations Residuals (Observed-Predicted) Determined Over All Times and Locations for the Two Day Period 26-27 June 1974: (a) Ozone (b) Nitrogen Dioxide

observed for NO_2 and O_3 for all monitoring stations over the two day simulation. Table 4 presents a summary of the statistics used to evaluate the model performance.

An important criterion in evaluating an air pollution model is its ability to predict the observed concentration maxima. Table 5 shows a comparison of the magnitudes of the predicted and observed O_3 maxima for 27 June at those stations where the observed maxima exceeded 0.20 ppm and a comparison of the predicted and observed hour of the O_3 maximum at the same stations. The predicted times of occurrence of the O_3 maxima agree exactly or are at most one hour removed from those observed. Because the phasing of predicted O_3 concentrations depends on virtually all the physical and chemical processes involved, the close agreement between observed and predicted temporal behavior suggests that these processes are accurately portrayed relative to their temporal dynamics.

In summary, because the essential trends of the predictions and observations are in agreement and because the model components represent state-of-the-art knowledge of each aspect, we assume that the basic model framework is a valid representation of atmospheric concentration dynamics.

5. Publications Derived From Research Project

In this executive summary only a brief outline of the photochemical modeling project can be presented. Further details of

TABLE 4

Summary Statistics Determined Over All Times and Locations for 26-27 June 1974[a]

PERFORMANCE MEASURE	DEFINITION[b]	INTERPRETATION OF STATISTICAL TEST	RESULTS OF TEST: OZONE (O_3)	RESULTS OF TEST: NITROGEN DIOXIDE (NO_2)	EVALUATION OF MODEL PERFORMANCE
Mean of Residuals	$\mu_i = \frac{1}{nm} \sum_{j=1}^{n} \sum_{k=1}^{m} w_i(x_j,t_k)$	A measure of the average bias in the predictions can be inferred from this test. The criterion indicates whether the model predominantly over-or-under-predicts the observed concentration.	0.0019 ppm [3%][c]	0.0078 ppm [11%][c]	While the model exhibits a slight tendency towards underprediction, the bias is of the order of typical monitoring instrument errors.
Root Mean Square Error (RMSE) Centered about the Mean	$\sigma_i = \sqrt{\frac{1}{nm} \sum_{j=1}^{n} \sum_{k=1}^{m} [w_i(x_j,t_k) - \mu_i]^2}$	This test measures the average spread of the residuals and, more importantly, it is insensitive to any bias in the predictions.	0.0382 ppm	0.0348 ppm	These results provide a formal measure of the spread of the residual histograms presented in Figure 10.
Correlation Coefficient	$r_i = \frac{\frac{1}{nm} \sum_{j=1}^{n} \sum_{k=1}^{m} \nu_i(x_j,t_k)\eta_i(x_j,t_k)}{\sqrt{\frac{1}{(nm)^2} \left(\sum_{j=1}^{n} \sum_{k=1}^{m} \nu_i^2\right)\left(\sum_{j=1}^{n} \sum_{k=1}^{m} \eta_i^2\right)}}$ where $\nu_i(x_j,t_k) = c_i^p(x_j,t_k) - \overline{c}_i^p$, $\eta_i(x_j,t_k) = c_i^o(x_j,t_k) - \overline{c}_i^o$ and $\overline{c}_i = \frac{1}{nm} \sum_{j=1}^{n} \sum_{k=1}^{m} c_i(x_j,t_k)$	The correlation coefficient measures the degree to which the magnitude of the predictions increase linearly with the magnitude of the observations. From a practical point of view it is important to note that the coefficient is insensitive to the extent of the increase. For example, if the predictions increase linearly at 1/10th of the rate of the observations then r will still be one.	0.89	0.67	For ozone (O_3) the predicted performance is excellent. In the case of nitrogen dioxide (NO_2) it is not possible to ascertain whether the low value of r is due to the model performance or interference from $HONO_2$ and PAN in the measurement of NO_2 (Adema, 1979; Higuchi et al., 1976).
Linear Least Squares Curve Fit	$c_i^p = \theta_i c_i^o + \phi_i$ where the slope θ_i is given by $\theta_i = \frac{\frac{1}{nm} \sum_{j=1}^{n} \sum_{k=1}^{m} \nu_i(x_j,t_k)\eta_i(x_j,t_k)}{\frac{1}{nm} \sum_{j=1}^{n} \sum_{k=1}^{m} \nu_i^2(x_j,t_k)}$ and intercept ϕ_i by $\phi_i = \overline{c}_i^o - \theta_i \overline{c}_i^p$	This performance measure can be used to assess the average increase in the predictions as the observations are increased. The slope parameter of the linear least squares curve fit is this measure. If the slope is nearly equal to one then the intercept is an indication of the bias.	slopes 0.851 intercepts 0.0115 ppm	0.709 0.0262 ppm	Both the slopes and intercepts for ozone (O_3) and nitrogen dioxide (NO_2) indicate that the model satisfactorily reproduces the observed concentration distributions.
Accuracy of Peak Prediction	$\frac{\max c_i^p(x_j,t_k)}{\max c_i^o(x_j,t_k)}$	Ratio of the maximum predicted peak concentration to the highest measured value.	$\frac{0.41}{0.51} = 0.80$	$\frac{0.31}{0.36} = 0.80$	For both ozone (O_3) and nitrogen dioxide (NO_2) the predicted highest concentrations are within 20% of the observations.
Timing of Peak Concentration Predictions	$\Delta t_i = t^o(x_j) - t^p(x_j)$	Difference in timing of predicted and observed peaks at the monitoring site with the highest observed concentration.	0 hrs[d]	-2 hrs[d]	As seen in Table 9 the predicted and observed ozone (O_3) concentration peaks were coincident at most monitoring sites. Differences of up to three hours were noted in the predicted times of the NO_2 peaks.
Error Bands	% of residuals over all j,k that satisfy $\lvert w_i(x_j,t_k)\rvert \leq$ bound	This measure gives the percentage of predictions that fall within a particular concentration bound.	83.8%[e]	88.9%[e]	Most of the residuals were within the $\pm$ 0.05 ppm concentration band.

Footnotes:

(a) In the statistical evaluation of model performance 1336 pairs of predictions and observations were used in the analysis of ozone (O_3) and 973 for nitrogen dioxide (NO_2).

(b) The residual for species i at locations j=1,2,...m and times k=1,2,...,m are defined as $w_i(x_j,t_k) = c_i^o(x_j,t_k) - c_i^p(x_j,t_k)$ where c_i^o and c_i^p are respectively the observed and predicted concentrations of species i.

(c) The values in brackets express the residuals as a percentage of the observed mean concentration. For ozone (O_3) the observed and predicted means were 0.0661 and 0.0641 ppm and for nitrogen dioxide (NO_2) 0.0709 and 0.0630 ppm respectively.

(d) The peak observed value of ozone (O_3) = 0.51 ppm occurred at Upland at 14:00 PST and the highest nitrogen dioxide (NO_2) = 0.36 ppm at downtown Los Angeles at 10:00 PST.

(e) Concentration bound set to $\pm$ 0.05 ppm .

TABLE 5

Observed and Predicted Maximum 1-hr Ozone Concentrations at SCAB Stations Where $[O_3]$ > 0.20 ppm and Timing of Ozone Maxima, 27 June 1974

	$[O_3]$, ppm		Time of maximum	
Station	Observed	Predicted	Observed	Predicted
Anaheim	0.23	0.21	1600	1600
La Habra	0.31	0.27	1500	1500
Los Alamitos	0.24	0.22	1700	1600
Norco-Prado Park	0.24	0.21	1600	1600
Riverside-Rubidoux	0.30	0.24	1500	1500
Riverside-Magnolia Avenue	0.24	0.24	1500	1500
San Bernardino	0.32	0.23	1500	1500
Chino	0.27	0.25	1400	1400
Upland-Civic Center	0.51	0.41	1600	1500
Upland-ARB	0.46	0.41	1500	1500
Fontana	0.49	0.38	1300	1400
Azusa	0.35	0.29	1200	1200
Burbank	0.30	0.30	1400	1300
Pomona	0.35	0.32	1100	1200
Whittier	0.38	0.30	1300	1200
Pasadena	0.31	0.31	1200	1200

the development and testing of the modeling system can be found in the open literature references cited in Table 6.

6. Conclusions

The major contribution of this research project has been the development of a mathematical modeling system that can be used to describe urban-scale photochemical air pollution. Based on the species continuity equation each model incorporates the combined influences of advective transport, turbulent diffusion, chemical reactions, source emissions and surface removal processes. Satisfactory performance of the modeling system has been demonstrated by comparing predicted and observed air quality over the South Coast Air Basin for the two day period 26-27 June 1974. The model predictions of the spatial and temporal variations of nitrogen dioxide (NO_2) and ozone (O_3) agree quite closely with measured air quality. These results and other tests indicate that the modeling system can now be used to evaluate air quality impacts of alternative emission control strategies.

TABLE 6

Summary of Publications from Photochemical Modeling Project

TOPIC	REFERENCE
General	
Model Development	McRae (1979, 1981) Goodin et al. (1979a) McRae et al. (1979, 1982ac)
Model Evaluation	McRae and Tilden (1980) McRae and Seinfeld (1982)
Applications	Seinfeld and McRae (1979) McRae (1980a)
Chemical Mechanism	
Mechanism Development	Falls and Seinfeld (1978) McRae et al. (1982a)
Sensitivity Analysis	Koda et al. (1979) Falls et al. (1979) Tilden et al. (1980) McRae et al. (1982d) McRae and Tilden (1980)
Water Vapor Concentration	McRae (1980b)
Objective Analysis Procedures	
Interpolation Techniques	Goodin et al. (1979b, 1981)
Wind Field Generation	Goodin et al. (1979c) Goodin and McRae (1980)
Turbulent Diffusion	
K-Theory Model	McRae et al. (1982a)
Convective Mixing	McRae et al. (1981)
Numerical Analysis	
Solution of the Atmospheric Diffusion Equation	McRae et al. (1982b)

Acknowledgements

The California Air Resources Board Research Division, its chief Dr. John Holmes, and the Air Quality Modeling Section: Andrew Ranzieri, Paul Allen, Praveen Amar, Marna Johns, Kit Wagner and Timothy Woody have contributed immeasurably to the success of this venture. Financial support for the work was provided by the California Air Resources Board contracts A5-046-87 and A7-187-30. Additional funding was provided by the U.S. Environmental Protection Agency Grant No. R805537 and a Department of Energy Institutional Grant EY-76-G-03-1305. Additional contributions were made by J.W. Tilden of the Environmental Quality Laboratory.

PUBLICATIONS LIST

Falls, A.H. and J.H. Seinfeld (1978) "Continued Development of a Kinetic Mechanism for Photochemical Smog," Environmental Science and Technology, 12, 1398-1406.

Falls, A.H., G.J. McRae and J.H. Seinfeld (1979) "Sensitivity and Uncertainty of Reaction Mechanisms for Photochemical Air Pollution," Int. J. Chemical Kinetics, 11, 1137-1162.

Goodin, W.R. and G.J. McRae (1980) "A Procedure for Wind Field Construction from Measured Data which Utilizes Local Surface Roughness," Proc. American Meteorological Society 2nd Conference on Coastal Meteorology, January, Los Angeles, California.

Goodin, W.R., G.J. McRae and J.H. Seinfeld (1979a) "Validity and Accuracy of Atmospheric Air Quality Models," Proc. American Meteorological Society: Third Symposium on Atmospheric Turbulence, Diffusion and Air Quality, October, Raleigh, North Carolina.

Goodin, W.R., G.J. McRae and J.H. Seinfeld (1979b) "A Comparison of Interpolation Methods for Sparse Data: Application to Wind and Concentration Fields," J. Applied Meteorology, 18, 761-771.

Goodin, W.R., G.J. McRae and J.H. Seinfeld (1979c) "An Objective Analysis Technique for Constructing Three-Dimensional, Urban-Scale Wind Fields," J. Applied Meteorology, 19, 98-108.

Goodin, W.R., G.J. McRae and J.H. Seinfeld (1981) "Reply to Comments on `A Comparison of Interpolation Methods for Sparse Data: Application to Wind and Concentration Fields,'" J. Applied Meteorology, 20, 92-94.

Koda, M., G.J. McRae and J.H. Seinfeld (1979) "Automatic Sensitivity Analysis of Reaction Mechanisms," Int. J. Chemical Kinetics, 11, 427-444.

McRae, G.J. (1979) "Mathematical Modeling of Photochemical Air Pollution," Proc. AIAA Symposium on Society and Aerospace Technology, Los Angeles, November 15.

McRae, G.J. (1980a) "Pollution and Pixels," A 16 mm color film on applications of digital image processing to air pollution. Produced by the Environmental Quality Laboratory in cooperation with the Jet Propulsion Laboratory, California Institute of Technology.

McRae, G.J. (1980b) "A Simple Procedure for Calculating Atmospheric Water Vapor Concentration," J. of the Air Pollution Control Association, 30 p. 394.

McRae, G.J. (1981) "Mathematical Modeling of Photochemical Air Pollution," Ph.D. Thesis, California Institute of Technology, Pasadena, California.

McRae, G.J., W.R. Goodin and J.H. Seinfeld (1979) "Development of a Second-Generation Airshed Model for Photochemical Air Pollution," Proc. American Meteorological Society, Fourth Symposium on Atmospheric Turbulence, Diffusion and Air Quality, January, Reno, Nevada.

McRae, G.J., W.R. Goodin and J.H. Seinfeld (1982a) "Development of a Second Generation Mathematical Model for Urban Air Pollution: I Model Formulation," Atmospheric Environment, 16, 679-696.

McRae, G.J., W.R. Goodin and J.H. Seinfeld (1982b) "Numerical Solution of the Atmospheric Diffusion Equation for Chemically Reacting Flows," J. Computational Physics, 45, 1-42.

McRae, G.J., W.R. Goodin and J.H. Seinfeld (1982c) "Mathematical Modeling of Photochemical Air Pollution," Final Report to the California Air Resources Board under contracts A5-046-87 and A7-187-30, Environmental Quality Laboratory, Report No. 18, California Institute of Technology, Pasadena, California, 800 pp.

McRae, G.J. and J.H. Seinfeld (1982) "Development of a Second-Generation Airshed Model for Urban Air Pollution: II Evaluation of Model Performance, Atmospheric Environment, submitted for publication.

McRae, G.J., F.H. Shair and J.H. Seinfeld (1981) "Convective Downmixing of Plumes in a Coastal Environment," J. Applied Meteorology, 20, 1312-1324.

McRae, G.J. and J.W. Tilden (1980) "Sensitivity and Uncertainty Analysis of Urban-Scale Air Pollution Models," Proc. American Meteorological Society Joint Conference on Applications of Air Pollution Meteorology, March 24-27, 1980, New Orleans.

McRae, G.J., J.W. Tilden and J.H. Seinfeld (1982d) "Global Sensitivity Analysis - A Computational Implementation of the Fourier Amplitude Sensitivity Test (FAST)," Computers and Chemical Engineering, 6, 15-25.

Seinfeld, J.H. and G.J. McRae (1979) "Use of Models to Establish Source-Receptor Relationships and Relative Source Contributions of NO_x to Air Quality," Proc. EPA Symposium on Implications of Low NO_x Vehicle Emission Standard, Washington, D.C. May 4.

Tilden, J.W., V. Costanza, G.J. McRae and J.H. Seinfeld (1980) Sensitivity Analysis of Chemically Reacting Systems", Proc. Workshop on Modelling of Chemical Reaction Systems, Heidelberg, Germany, September 1-5. Sponsored by Sonderforschungsbereich 123, Stochastische Mathematische Modelle, University of Heidelberg.